

---

## Abstract

Increasing the share of electricity produced from renewable energy sources (RES), combined with RES dependence on weather, poses a critical challenge for energy systems. This study investigates the importance of the balance between wind and photovoltaic (PV) capacity on periods of low renewable generation, known as RES droughts. Three different RES models are used to estimate the capacity factors for different scenarios of installed capacities for wind and PV power. The skill of the RES models is quantified by comparing capacity factor time series to observed hourly data and by assessing their representation of observed RES droughts. The RES models are used to generate a 45-year hourly time series of RES capacity factor, enabling analysis of the frequency, duration and return periods of RES droughts at a climatological scale. Results show the importance of using an accurate, validated RES model for RES drought risk assessment. The addition of PV capacity to a wind-dominated system results in a significant reduction in the frequency and duration of RES droughts, while also reducing extremes and seasonal drought patterns. These findings underscore the importance of diversification in RES capacity to enhance energy security and resilience.

*Keywords:* RES Drought, Wind Power, Solar PV Power, Renewable Energy Sources, Return Periods

---

## 1. Introduction

The EU aims to generate at least 69% of its electricity from renewable energy sources (RES) by 2030, up from 41% in 2022 [1]. While this transition is essential for reducing greenhouse gas emissions, it also highlights the challenge of managing the variability of weather-dependent energy sources such as wind and photovoltaic (PV) power. This challenge is compounded by the increasing electrification of energy sectors, which places greater demand on the power system and makes it more sensitive to meteorological conditions [2, 3, 4]. Periods of low renewable generation, known as *Dunkelflaute* or RES droughts, pose significant risks to system adequacy and energy security, emphasising the need for a resilient energy system to meet both growing electricity demand and decarbonisation targets.

This study focuses on Ireland, a region with a strong reliance on wind power, which has ambitious targets for PV power expansion. This case study

provides valuable insights into the potential benefits of diversifying the renewable energy mix on RES droughts. The performance of different RES models are compared, and a 45-year time series of RES generation is produced. The results highlight the role of increased PV capacity in reducing RES drought risks, offering insights for policymakers and energy planners.

For this study, a RES drought event is defined as occurring when the average capacity factor (CF) remains below a fixed threshold for a given duration, following the methodology used in other research [5, 6, 7, 8]. Alternative methods exist for defining RES droughts. One approach uses relative CF thresholds that change over the year to account for seasonal variations in renewable energy generation [9, 10, 11, 12, 13]. Another common method relies on percentile-based thresholds, where drought events are defined by identifying periods of unusually low generation relative to historical production levels, typically based on the lowest production percentiles [12, 14]. Additionally, some studies combine these definitions with metrics that incorporate the demand side of energy consumption, analysing the balance between supply and demand during drought periods [9, 10, 12, 14]. In this paper, the focus is exclusively on energy generation, and a fixed threshold approach to define RES droughts is used, which facilitates consistent inter-comparison between scenarios with different installed wind and PV capacities.

RES droughts are identified using onshore wind and PV CF time series. In this study, three different datasets are used, all of which are driven by ERA5 data [15]. Two of the datasets are part of C3S Energy (C3S-E), an energy-based operational dataset produced by the EU Copernicus Climate Change Service [16, 17]. One of the C3S-E datasets provides CF time series aggregated at the national scale, while the other provides the CF time series at each grid point, at the ERA5 resolution of  $0.25^\circ$ . The third dataset was generated using the Atlite model [18], which converts the ERA5 atmospheric data to a generation time series using specified wind turbine and PV panel models. Atlite is an open-source tool developed by PyPSA [18] and is widely used for estimating wind and PV generation [7, 19, 20, 21].

The datasets used in this study are detailed in section 2, which describes their characteristics and relevance for evaluating RES droughts. Section 3 outlines the RES models used to simulate wind and PV generation and provides the methodology for defining and identifying RES drought events, including the thresholds and metrics applied. In section 4, the models are first verified against observed energy data to assess their accuracy, followed by an analysis of RES drought occurrences for two scenarios with different ratios

53 of installed wind to PV capacities. Finally, section 5 offers a discussion of  
54 the results in the context of energy reliability and future planning, followed  
55 by the main conclusions and recommendations for further research.

## 56 **2. Data**

57 This study uses publicly available datasets to construct and validate the  
58 models for estimating the CF of wind and PV energy. The primary data  
59 sources include: EirGrid and SONI, the transmission system operators (TSO)  
60 for the Republic of Ireland and Northern Ireland, respectively; the ERA5  
61 reanalysis dataset; and the C3S-E datasets.

### 62 *2.1. Wind and PV Capacity and Availability*

63 EirGrid, the TSO for the Republic of Ireland, and SONI, the Northern  
64 Ireland TSO, provide detailed datasets on all wind and PV farms across the  
65 island of Ireland (Republic of Ireland and Northern Ireland) from 1990 to the  
66 present [22]. These datasets include information such as each farm’s installed  
67 capacity, name, and connection date. To enhance the accuracy of this data,  
68 the longitude and latitude for each farm were manually determined through  
69 online searches. For simplicity, this data will be referred to as originating  
70 from EirGrid, as all-island data was directly obtained from EirGrid, and the  
71 combined regions of the Republic of Ireland and Northern Ireland will be  
72 referred to as Ireland throughout the remainder of this document.

73 The spreadsheet available from the EirGrid website contains two key vari-  
74 ables: generation and availability. Generation is the energy that a RES farm  
75 actually contributed to the grid, which may include limitations introduced  
76 by the TSO to maintain grid stability, such as constraints and curtailment.  
77 Availability represents the energy that would have been generated from a  
78 RES farm if no grid constraints had been applied, making it representative  
79 of the weather-related response. Generation and availability values are avail-  
80 able from 2014 onward for wind power and from 2018 onward for PV power,  
81 although PV availability data only became present in the Republic of Ireland  
82 in 2023. This study focuses on availability for all analyses.

### 83 *2.2. Atmospheric Variables*

84 Atlite and C3S-E datasets are driven by the ERA5 reanalysis [15], pro-  
85 duced by the European Centre for Medium-Range Weather Forecasts (ECMWF).  
86 This global gridded dataset provides hourly atmospheric variables from 1940

87 to the present at a horizontal resolution of  $0.25^\circ$ . It is widely used for esti-  
88 mating PV and wind energy [7, 16, 23, 24]. Table 1 lists the ERA5 variables  
89 used by Atlite and C3S-Energy.

Table 1: ERA5 variables used to calculate wind and PV generation

ERA5 name	variable
100 metre zonal and meridional wind speed	$u_{100}, v_{100}$
2 metre temperature	$t2m$
Surface net solar radiation	$ssr$
Surface solar radiation downwards	$ssrd$
Top of atmosphere incident radiation	$tisr$
Total sky direct solar radiation at surface	$fdir$

### 90 2.3. C3S Energy

91 The EU Copernicus Climate Change Service developed the C3S-E renew-  
92 able energy dataset for Europe [16], using ERA5 atmospheric variables and  
93 weather-to-energy models. This dataset provides hourly CF for wind and PV  
94 energy from 1979 to the present. The data are available on the same grid as  
95 the ERA5 data, which has a horizontal resolution of  $0.25^\circ$ . The time series  
96 are also available for download at two aggregated scales: regional (NUTS 2)  
97 and national.

98 The C3S-E dataset estimates wind energy using wind speeds at 100 me-  
99 tres ( $u_{100}, v_{100}$ ) and a standard turbine model, the Vestas V136/3450, with  
100 a fixed hub height of 100 meters. This choice is based on expert advice and  
101 the trend in wind turbine installation. The PV generation model used by  
102 C3S-E uses two ERA5 variables: surface solar radiation downwards ( $ssrd$ )  
103 and air temperature ( $t2m$ ). PV generation is calculated multiple times, us-  
104 ing the same model with different azimuth and tilt angles. The results are  
105 aggregated based on a statistical distribution of the module angles based on  
106 the geographical location [25].

## 107 3. Methods

108 This study uses three datasets to analyse RES droughts across the island  
109 of Ireland. Data downloaded from C3S-E were used to obtain two datasets:  
110 one based on national-level data (C3S-E N), and another on grid-level data  
111 (C3S-E G). The third dataset was computed using the Atlite model (Atlite).

### 112 3.1. C3S-Energy National

113 For national-level analyses, the aggregated CF time series provided by  
114 C3S-E were used at two levels: Republic of Ireland (NUTS0: IE) and North-  
115 ern Ireland (NUTS2: UKN0). These are based on the assumption by C3S-E  
116 that RES generation occurs at every ERA5 grid point in Ireland. We com-  
117 puted a weighted average of these, based on the installed capacity of each  
118 one, to represent the total CF for Ireland.

### 119 3.2. C3S-E Gridded

120 The gridded dataset from C3S-E was used to create CF datasets which  
121 account for the location of RES farms in Ireland. A list of the RES farms in  
122 Ireland was compiled, including each farm’s latitude, longitude and installed  
123 capacity. Using these coordinates, the nearest grid point on the C3S-E grid  
124 was identified for each farm. The CF values from the C3S-E dataset corre-  
125 sponding to these grid points were retrieved. A weighted average of the CF  
126 values was calculated, with the installed capacity of each farm serving as the  
127 weight, to construct the CF time series for Ireland. This process resulted in  
128 a time series of RES generation for each energy source (wind and PV) for  
129 Ireland, which takes the location of the RES farms into account.

### 130 3.3. Atlite

131 Atlite transforms weather data into energy data using the gridded ERA5  
132 data and the locations of existing RES farms, as described in C3S-E G.  
133 ERA5 data for wind speed at 100 metres ( $u_{100}$ ,  $v_{100}$ ) are used to calculate  
134 wind generation, while the ERA5 radiation variables ( $ssr$ ,  $ssrd$ ,  $tisr$ , and  
135  $fdir$ ) and air temperature ( $t2m$ ) are used to calculate PV generation. A  
136 key distinction between C3S-E and Atlite lies in their representation of wind  
137 turbines and PV panels. This study identifies the most appropriate wind  
138 turbine power curve to use from the 121 power curves made available by  
139 Renewables.ninja [26]. The selection of a specific wind turbine and PV panel  
140 characteristics is further discussed and explained in section 4.1.

### 141 3.4. Energy Scenarios

142 In addition to analysing wind and PV generation separately, a combined  
143 CF was computed for each model by averaging wind and PV generation,  
144 weighted by their installed capacities at the end of 2023 (5.9 GW for wind  
145 power and 0.6 GW for PV power). This configuration is referred to as the

146 91W-9PV scenario, reflecting the distribution of 91% wind and 9% PV ca-  
 147 pacity. Given that PV capacity in Ireland is low in 2023, and to explore how  
 148 a more balanced distribution of wind and PV capacities might impact RES  
 149 droughts, this study also considered a second scenario, referred to as 57W-  
 150 43PV, where the installed PV capacity is assumed to increase to 8.6 GW,  
 151 while wind capacity rises to 11.45 GW. These values are based on targets  
 152 outlined in the roadmap published by the 2024 Climate Action Plan [27].  
 153 This study does not include offshore wind in the analysis. Recent reports  
 154 suggest that even by 2030, Ireland is unlikely to have any significant new off-  
 155 shore wind farms, with projected offshore capacity expected to remain near  
 156 zero using realistic scenarios [28].

157 New time series were generated for both the Atlite and C3S-E G PV mod-  
 158 els, incorporating a revised distribution of installed capacity across Ireland  
 159 as specified in the roadmap. For wind power, the CF time series remains un-  
 160 changed, as significant shifts in the location of wind farms are not expected.  
 161 In total, twelve CF time series were analysed in this study, six for individual  
 162 wind and PV CF (three models for each source) in the 91W-9PV scenario,  
 163 and an additional six time series that include the combined CF for 91W-9PV  
 164 and 57W-43PV scenarios across the different models.

165 It is important to note that the specific capacity values used in this study  
 166 are illustrative and are not intended to reflect precise future realities. Instead,  
 167 they serve to explore the impact of transitioning from a wind-dominated sys-  
 168 tem (91W-9PV) to a more evenly distributed system (57W-43PV). This ap-  
 169 proach allows for a comparative analysis between the two scenarios, assessing  
 170 how the balance of RES capacity affects the occurrence of RES droughts.

### 171 3.5. *RES Drought Definition*

172 In this study, a RES drought event was defined as occurring when the  
 173 24-hour moving average of CF remains below a fixed threshold of 0.1 for  
 174 a period of longer than 24 hours. The choice of this threshold is somewhat  
 175 arbitrary, but aligns with similar studies on low renewable energy production  
 176 [5, 6, 8]. By using a 24-hour moving average, fewer but longer-lasting events  
 177 were captured compared to using the raw CF time series, which can be more  
 178 sensitive to short-term fluctuations. A fixed threshold approach was chosen  
 179 in this study to enable consistent inter-comparison between datasets.

180 The moving average approach smooths out short-term fluctuations, so  
 181 that brief periods above the threshold do not interrupt an otherwise con-  
 182 tinuous low-CF period (Fig. 1). This means that a single hour above the

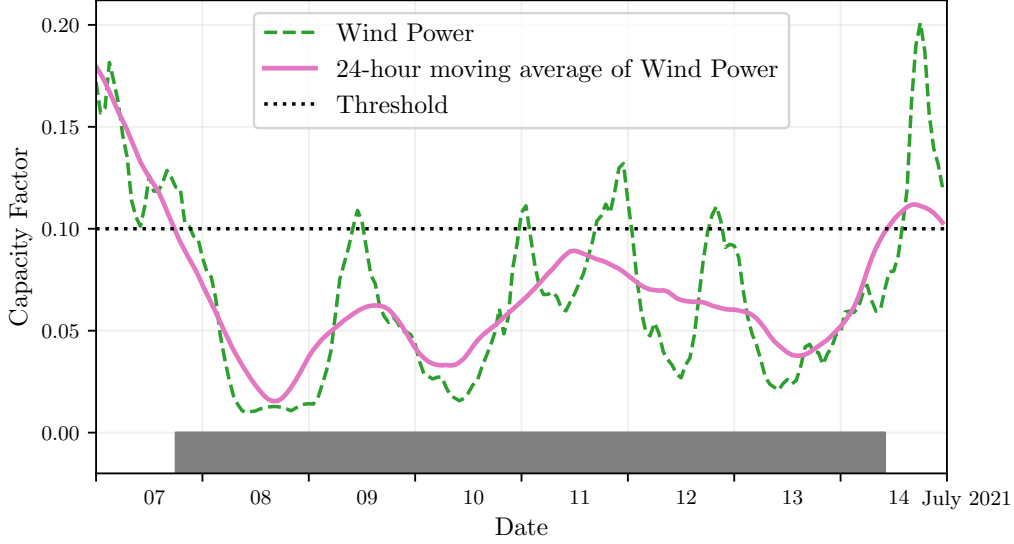


Figure 1: Wind time series of CF (green) and its 24-hour moving average (pink) from the 7th to the 15th of July 2021. The black dashed line indicates the CF threshold. The grey bar shows the period identified as a wind drought under our definition

threshold does not "break" a drought event if it is surrounded by prolonged  
low-generation hours. As a result, fewer but longer-lasting drought events  
are identified, which may better reflect real-world conditions where energy  
supply constraints persist over extended periods.

## 4. Results

### 4.1. Verification

The accuracy of the datasets used in this study was verified, before continuing to the analysis of RES droughts. For the verification process, time-varying values of installed capacity were used to account for changes in RES development over the verification period. This step allowed us to assess how well the datasets represent the production of renewable energy by comparing them against observed data.

#### 4.1.1. Wind Energy

The C3S-E datasets use the Vestas V136/3450 wind turbine power curve, (Fig. 2a). The Atlite model allows the user to specify the power curve.

198 We considered the 121 power curves available for download from Renew-  
 199 ables.ninja [26]. For each power curve, Renewables.ninja also provides four  
 200 associated smoothed power curves. The smoothing is done using a Gaussian  
 201 filter with different standard deviations that depend on the wind speed. A  
 202 separate wind CF time series for Ireland was generated for each of the wind  
 203 turbine power curves and smoothing levels. The performance of each CF  
 204 time series was then assessed based on four skill scores: correlation coeffi-  
 205 cient (CC), root mean square error (RMSE), mean bias error (MBE), and  
 206 area under the curve (AUC). The AUC was calculated from histograms of  
 207 the hourly CF values for the most recent decade, 2014-2023. Based on these  
 208 metrics, the most representative power curve for Ireland was the Enercon  
 209 E112.4500 power curve with the  $0.3w$  smoothing filter.

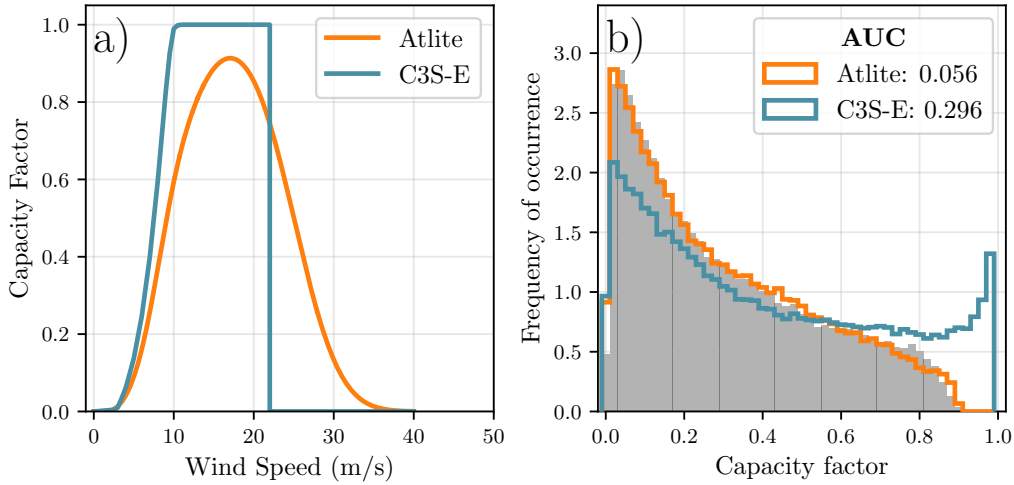


Figure 2: a) Power curves of the Enercon E112.4500 with a  $0.3w$  smoothing filter used by  
 Atlite (orange) and the Vestas V136/3450 used by C3S-E (blue) b) Histograms of wind  
 CF for Ireland from Atlite (orange), C3S-E (blue) and Observed (shaded)

210 The smoothing of the wind turbine power curve represents losses associ-  
 211 ated with each turbine, as well as losses such as wake effects between turbines,  
 212 which are important when modelling wind energy on larger spatial scales.  
 213 The histogram in Fig. 2b shows that the C3S-E power curve tends to under-  
 214 estimate low CF values and overestimate higher ones, whereas the smoothed  
 215 Atlite power curve more closely follows the observed wind availability data.  
 216 This is further supported by the AUC - a negatively oriented skill score -



217 which is lower for Atlite than for C3S-E, indicating better alignment with  
 218 observed data.

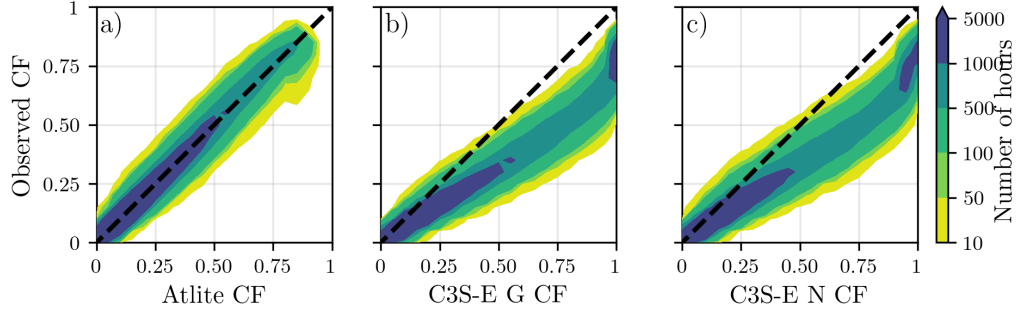


Figure 3: Wind CF density plot of the observed CF (vertical axes) and modelled (horizontal axes) CF data for the a) Atlite, b) C3S-E G and c) C3S-E N models

219 The effect of the difference between the power curves is also visible in  
 220 Fig. 3, which shows a density plot of wind CF values. The two C3S-E datasets  
 221 are shown to overestimate the observed CF, whereas the Atlite model is in  
 222 good agreement with the observed data. The skill scores presented in Table 2  
 223 show that Atlite performs better than the C3S-E datasets for all of the skill  
 224 scores.

	Atlite	C3S-E G	C3S-E N
<b>CC</b>	0.981	0.972	0.970
<b>RMSE</b>	0.045	0.177	0.162
<b>MBE</b>	-0.003	0.137	0.121

Table 2: Skill scores for wind power for the three datasets compared to observed data

225 Fig. 4 shows the average annual number of wind drought events during  
 226 the 2014 to 2023 validation period. The figure reveals that Atlite presents  
 227 the best overall agreement with the observed frequency and duration of wind  
 228 drought events. This pattern is particularly evident for shorter-duration  
 229 events, which are the most frequent.

#### 230 4.1.2. PV Energy

231 The Atlite model allows the user to select certain PV panel characteristics.  
 232 In this study, the three PV panel types available in the Atlite model were

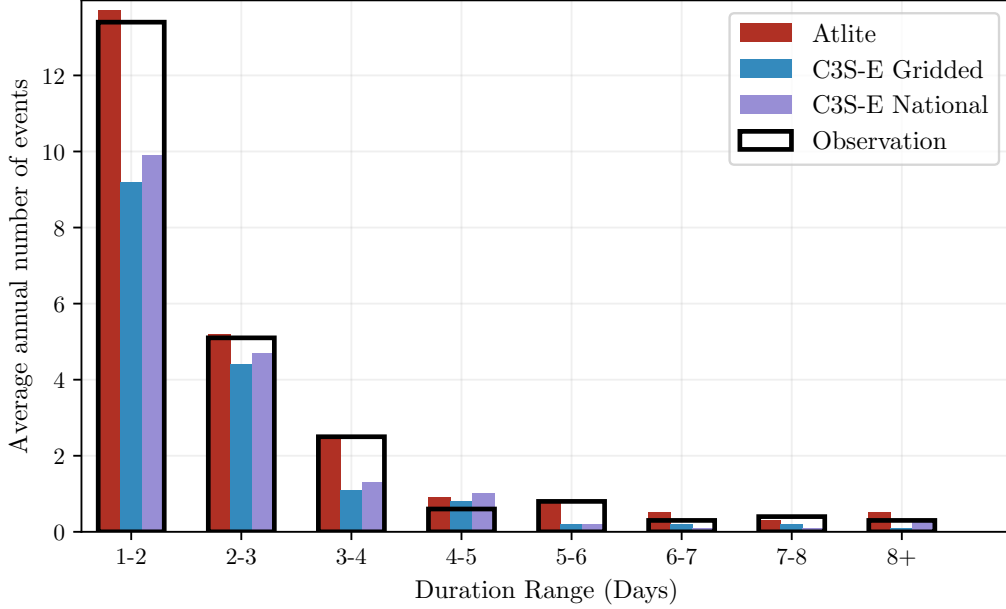


Figure 4: Average annual number of wind drought events for Atlite (red), C3S-E G (blue), C3S-E N (purple), and the observed data (black outline). The wind droughts are identified from 2014 to 2023, considering the actual capacity of the system at any given time

considered (CSi, CdTe, Kaneka). Following the same methodology as in the previous section, the three available models were compared using four skill scores (CC, RMSE, MB, and AUC). Based on the best-performing metrics, the Breyer PV panel model was selected [29], using the Kaneka Hybrid panel option. For all PV farm locations, the azimuth angle is fixed at  $180^\circ$  (due south), and the optimal tilt angle option is applied.

The PV installed capacity available on the spreadsheets from EirGrid represents the Maximum Export Capacity (MEC) and does not accurately reflect the installed PV capacity. To enable actual PV generation potential to be modelled correctly, installed capacities were set at 1.4 times the MEC values. This scaling factor was estimated by analysing proprietary data from individual PV farms provided by EirGrid, which showed that, on average, assuming that the installed capacities of farms exceed their MEC values by 40% yields the best agreement with the observed availability.

Figure 5 shows that the three datasets have a similar tendency to overestimate the CF compared to the observed values, especially for high CF values.

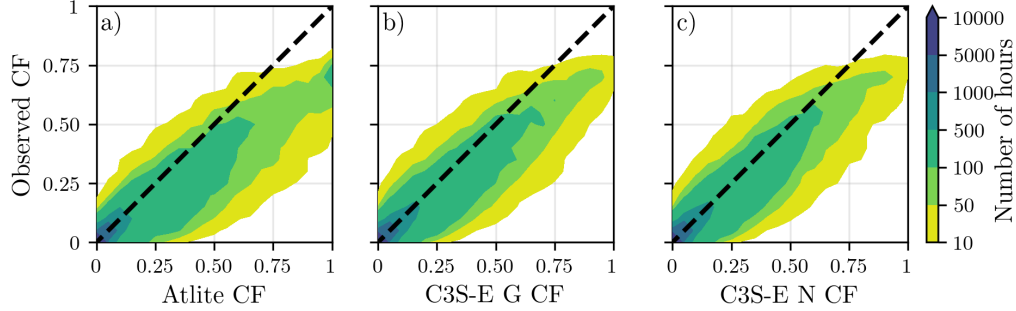


Figure 5: PV CF density plot of the observed (vertical axes) and modelled (horizontal axes) CF series for the a) Atlite, b) C3S-E G and c) C3S-E N models

249 The skill scores presented in Table 3 indicate that C3S-E G performs best  
 250 overall, with the lowest RMSE and a high correlation coefficient, suggesting  
 251 a closer match to observed data. All models show a slight positive bias, with  
 252 Atlite exhibiting a slightly lower correlation and higher RMSE.

	Atlite	C3S-E G	C3S-E N
<b>CC</b>	0.921	0.931	0.931
<b>RMSE</b>	0.119	0.090	0.113
<b>MBE</b>	0.046	0.027	0.021

Table 3: Skill scores for PV CF for the three datasets compared to observed data

253 Fig. 6 shows the number of PV drought events during the 2023 validation  
 254 period across different duration ranges. The figure reveals partial agreement  
 255 between the three datasets and the observed data, with consistent results  
 256 noticed for duration ranges of 1-2, 3-4, 7-8, and 8+ days. However, dis-  
 257 crepancies appear in the other ranges, where the models diverge from the  
 258 observed data. The main challenge in validating PV data stems from the  
 259 recent installation of a large share of Ireland’s PV capacity, with over 65% of  
 260 the total PV capacity installed in 2023. This results in uncertainties in PV  
 261 generation data and the actual generating capacity in the first few months  
 262 after each farm is connected.

263 As the goal of this analysis is to assess the combination of wind and PV  
 264 generation, the complementary nature of these energy sources mitigates the  
 265 limitations in PV-only results.

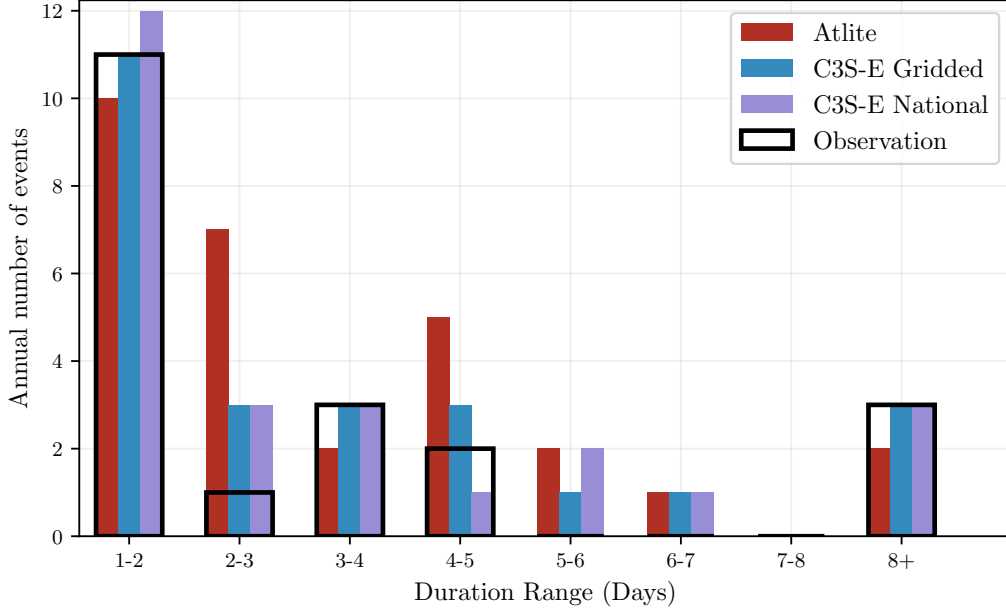


Figure 6: Number of PV drought events for Atlite (red), C3S-E G (blue), and C3S-E N (purple) and the observed data (black outline). The PV droughts are identified for 2023, considering the actual capacity of the system at any given time

#### 4.2. Analysis

In this section, RES drought events are evaluated under two different scenarios with fixed installed capacities: the 91W-9PV scenario, with 5.9 GW of wind capacity and 0.6 GW of PV capacity; and the 57W-43PV scenario, where wind capacity comprises 11.45 GW and PV capacity increases to 8.6 GW. Both scenarios were driven by 45 years of ERA5 data. Using the RES drought identification process described in Section 3.5, wind and PV droughts are first analysed separately before presenting the results for combined (wind + PV) RES droughts under both scenarios.

##### 4.2.1. Annual Number of RES Droughts

The first part of the analysis examines the annual number of RES drought events across the three datasets. When only wind energy is considered (Fig. 7a), the number of events decreases as the duration range increases, with very few events lasting more than seven days. In the case of only PV energy (Fig. 7b), the number of events also declines as the duration

range extends from one to eight days, followed by a slight increase for longer durations. This increase occurs because Ireland, being located above the 50° parallel, experiences reduced sunlight during the winter months. From November to March, PV output often remains consistently low, leading to extended periods where generation stays below the CF threshold.

When comparing wind and PV results (Fig. 7a & b), the median, first, and third quartiles for PV are consistently higher than or equal to those for wind, across all duration ranges and datasets. This is due to the typically lower CF of PV power compared to wind power, especially in a region such as Ireland where solar potential is limited. PV generation is also zero at night and constrained by the daily solar cycle, leading to a naturally higher frequency of drought events in PV compared to wind.

Fig. 7c & d show the combination of wind and PV under the two capacity scenarios. In the 91W-9PV scenario (Fig. 7c), the identified RES droughts closely match those for wind alone, which is expected due to the dominance of installed wind capacity. In contrast, the 57W-43PV scenario (Fig. 7d) shows a clear reduction in the number of drought events across all datasets and durations, with a decrease of the total number of events of 56% for Atlite, 52% for C3S-E G, and 50% for C3S-E N. This reduction is attributed to the anti-correlation between wind and PV generation.

The median, first, and third quartiles for the Atlite dataset are consistently greater than or equal to those of the other two datasets, regardless of the duration range or type of renewable energy considered. This difference arises from the wind turbine power curve model used in the C3S-E datasets, which tends to overestimate the wind CF (Fig. 3). As a result, the overall number of RES droughts is underestimated in the C3S-E datasets compared to Atlite.

#### 4.2.2. Return Periods of RES Drought Duration

The RES drought events identified over the 45-year period were used to calculate the return periods for different RES drought durations. A return period is the estimated average time interval between events of a specified duration or intensity (not to be confused with the frequency of their occurrence within a fixed time frame). Fig. 8 illustrates the return periods for varying RES drought durations, highlighting how often different drought lengths are likely to occur across the datasets. This analysis provides insight into the frequency and likelihood of prolonged low-generation periods, which is crucial for evaluating the potential impact of RES droughts on energy reliability

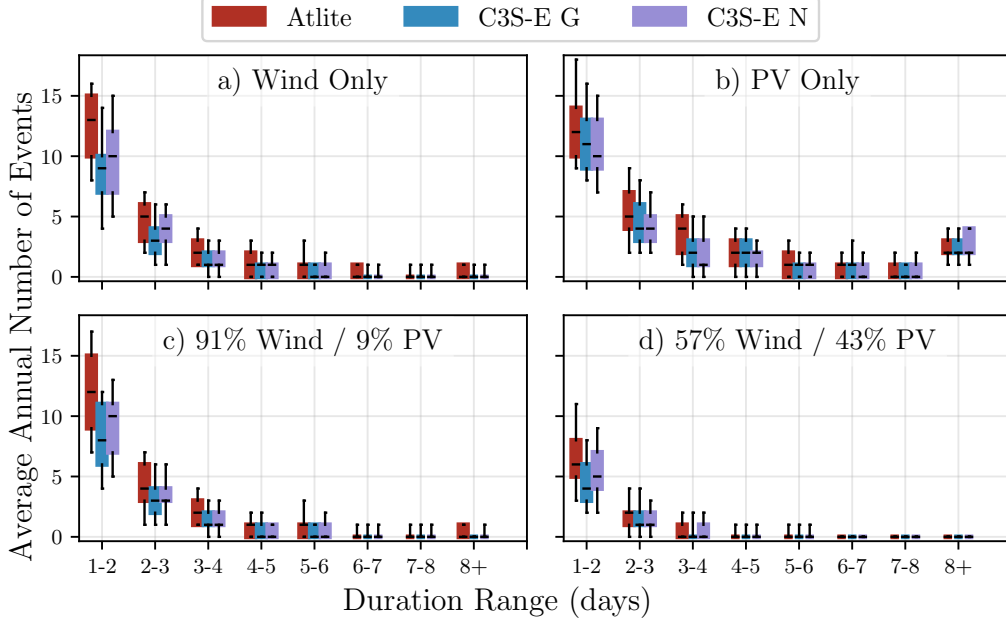


Figure 7: Average annual number of RES droughts (from 1979 to 2023) for a) Wind, b) PV, c) 91W-9PV and d) 57W-43PV for Atlite (red), C3S-E G (blue), and C3S-E N (purple). The x-axis represents duration ranges in days (lower bound included), while the y-axis indicates the annual number of events. The boxes display the first and third quartiles and the median is marked by a black line. The whiskers indicate the 5th and 95th percentiles

318 and security of supply.

319 The duration of wind droughts (Fig. 8a) increases in a log-linear fash-  
 320 ion across the three datasets. The log-linear trend indicates a predictable  
 321 relationship between drought duration and occurrence, with longer wind  
 322 droughts becoming exponentially less likely as duration increases.

323 In the case of PV droughts (Fig. 8b), Atlite behaves differently than the  
 324 two C3S-E datasets. The Atlite results show a generally log-linear increase.  
 325 For C3S-E G and C3S-E N, the duration of PV droughts increases in a log-  
 326 linear pattern for events lasting less than 16 days. Beyond this duration,  
 327 there is a sharp rise in drought duration for events up to a one-year return  
 328 period. This sudden increase again reflects the impact of extended periods  
 329 of low PV generation during winter in Ireland.

330 The difference between Atlite and the C3S-E results arises from differ-  
 331 ences in the datasets near the threshold of 0.1 CF. Atlite remains slightly

above the threshold more frequently during these conditions, leading to shorter, more fragmented drought events. In contrast, C3S-E G and C3S-E N tend to fall below the threshold in similar conditions, resulting in longer continuous drought periods, especially during winter.

For the 91W-9PV scenario (Fig. 8c), the return periods mirror those of Fig. 8a, due to the low levels of installed PV capacity. In the 57W-43PV scenario (Fig. 8d), the return periods for RES droughts increase across all durations. For example, the return period for a five-day drought event (shown by the vertical dashed lines in Fig. 8) extends from roughly six months for the 91W-9PV scenario, to four years for the 57W-43PV scenario in the Atlite dataset, and from about fifteen months to around five years in the two C3S-E datasets.

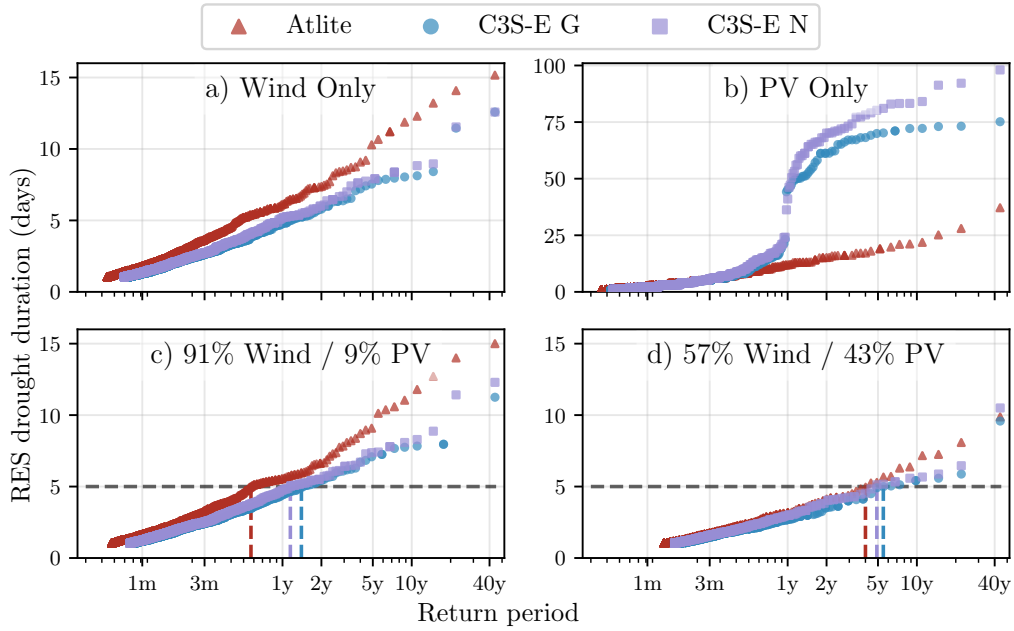


Figure 8: Return periods of the duration of RES droughts (from 1979 to 2023) for a) Wind, b) PV, c) 91W-9PV and d) 57W-43PV for Atlite (red triangle), C3S-E G (blue circle), and C3S-E N (purple square). The x-axis represents the return period time in a log-scale and the y-axis indicates the duration of RES drought associated with it. The horizontal dashed line marks the 5-day return period, with coloured vertical dashed marking its return period for each dataset

Across Fig. 8a, c, and, d, the return periods in the Atlite dataset are

consistently higher than those in the two C3S-E datasets. For instance, in the 91W-9PV scenario (Fig. 8c), an event with a one-year return period lasts six days in the Atlite dataset, compared to only five days in the C3S-E datasets. This difference underscores the importance of model selection when quantifying RES droughts, as each model’s assumptions and parametrisations significantly influence drought duration estimates. Additionally, in all four graphs, the similarity between results from the two C3S-E datasets suggests that assumptions in the Atlite model—such as wind turbine power curve selection and PV panel specifications—have a greater impact on RES drought duration estimates than the precise geographic distribution of RES farms when studying the return periods of RES droughts.

#### 4.2.3. Seasonal Distribution of RES Droughts

The seasonality of RES droughts was analysed by comparing the percentage of hours in each month classified as part of a RES drought.

For wind-dominated scenarios (Fig. 9a & c), the percentage of hours that are part of a drought is higher in summer than in winter. In the Atlite dataset, for instance, an average of 24% of hours in summer (June-July-August) are identified as wind droughts, compared to only 4% in winter (December-January-February). This seasonal variation is less prominent for the two C3S-E datasets compared to the Atlite one. This difference can be linked to the shape of the two power curves (Fig. 2). CFs near or under the 0.1 threshold occur at higher wind speeds for the Atlite power curve than for the C3S-E one. In contrast, the results for PV droughts (Fig. 9b) show a higher percentage in winter, with PV droughts occurring over 60% of the time regardless of the dataset. The Atlite results show a higher percentage of PV drought hours for wind, and a slightly lower percentage for PV, compared to the two C3S-E datasets.

The 91W-9PV scenario (Fig. 9c) shows patterns comparable to the ones for wind droughts (Fig. 9a). However, in the 91W/9PV scenario, the number of hours classified as RES droughts in summer decreases slightly compared to the wind-only scenario. This reduction can be explained by the contribution of PV generation during the summer months in the 91W-9PV scenario, even though it constitutes only 11% of total capacity. Since the number of RES drought hours for PV in summer is near zero, this small contribution has a noticeable impact on reducing overall drought hours. In the 57W-43PV scenario (Fig. 9d), all three datasets show a reduction in monthly RES drought frequency. Annual reductions in median RES drought frequency are observed



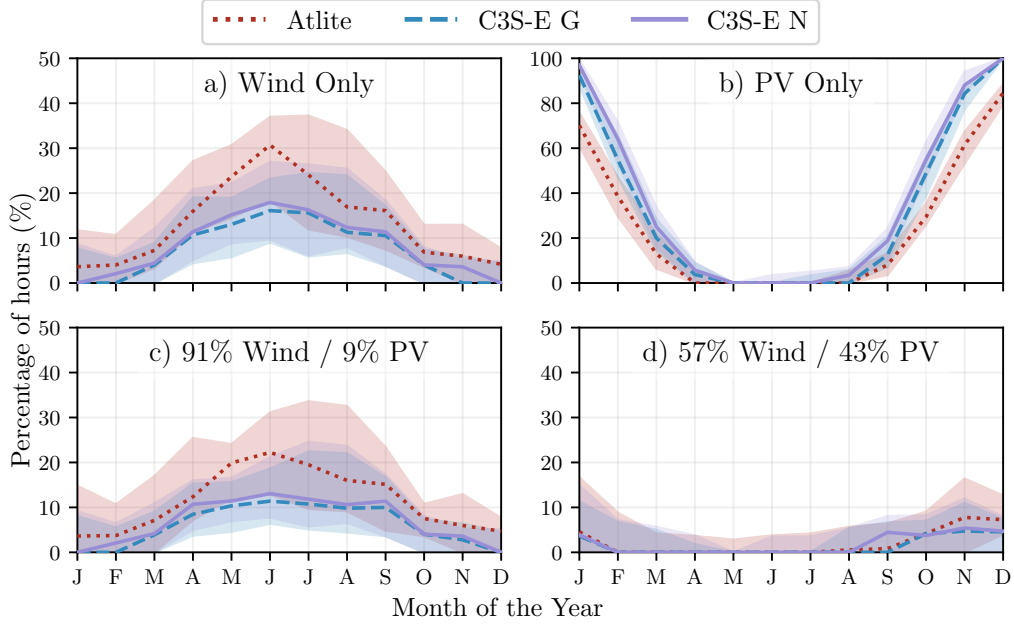


Figure 9: Percentage of hours in a month which are part of a RES drought (from 1979 to 2023) for a) Wind, b) PV, c) 91W-9PV and d) 57W-43PV for Atlite (red dotted), C3S-E G (blue dashed), and C3S-E N (purple solid). The x-axis represents the month of the year, and the y-axis indicates the percentage of hours. Lines correspond to the median values and the area between the first and third quartiles is shaded. Note the different y-axis scale for b).

across the datasets, dropping from 14% to 5% for Atlite, from 8% to 3% for C3S-E G, and from 9% to 4% for C3S-E N. The balanced mix of wind and PV power in this scenario reduces the seasonal signal overall and significantly decreases the percentage of RES drought hours in the summer.

## 5. Discussion and Conclusions

This study has investigated the ability of three RES models to represent RES droughts: Atlite, C3S-E G, and C3S-E N. One of the most evident differences is how each dataset incorporates the specific locations of RES farms. Both Atlite and C3S-E G consider the locations of wind and PV farms, which one would expect to result in a more accurate representation of RES generation. While this approach slightly improves PV models, our analysis indicates that for wind energy, the Atlite dataset performs better

394 overall, especially in its close alignment with observed data for wind gener-  
395 ation estimates. This finding suggests that, although the inclusion of RES  
396 farm locations is beneficial, the accuracy of the RES model is more strongly  
397 influenced by underlying model assumptions, such as selecting an appropriate  
398 wind power curve.

399 Atlite shows the best alignment with observed data for wind generation.  
400 Differences between the models are smaller for PV, with C3S-G performing  
401 marginally better than the other two. The results show that the two C3S-E  
402 datasets (C3S-E G and C3S-E N) consistently yield similar outcomes, indi-  
403 cating that their methodological differences have minimal impact. In this  
404 case, that distinction is also evident in the analysis, where Atlite reports  
405 higher return periods and a greater number of RES droughts, especially in  
406 scenarios with a balanced share of RES. Again, the results from RES drought  
407 modelling rely more on the precision of the wind power curve and PV panel  
408 models than on the specific locations of RES farms. Atlite’s superior perfor-  
409 mance highlights the importance of selecting validated models for assessing  
410 RES drought risks. This careful model selection can better quantify risks,  
411 support effective planning, and avoid the potential underestimation of ca-  
412 pacity needs, which is essential for ensuring energy security.

413 Looking at the 57W-43PV scenario, the analysis showed a significant im-  
414 provement in the management of RES droughts due to the complementary  
415 nature of wind and PV generation. Wind and PV together perform better  
416 in terms of reducing drought frequency and duration than either would in-  
417 dividually, largely because of the seasonal anti-correlation between the two  
418 energy sources. This diversification reduces the seasonal impact on RES  
419 droughts, as PV generation peaks in the summer and wind generation is  
420 more consistent in winter. Ireland currently has a highly wind-dependent  
421 energy system, but with ambitious targets for PV installations in the coming  
422 years, the energy mix is expected to approach a balance between wind and  
423 PV capacity. While this balanced approach offers a more stable and secure  
424 energy supply by mitigating RES drought risks, it is important to note that  
425 having similar wind and PV capacities may not optimise other aspects, such  
426 as annual energy production or meeting nighttime loads. For policymakers,  
427 these findings underscore the importance of meeting these capacity targets  
428 to enhance energy security through diversification. Additionally, the choice  
429 of model for RES drought assessment becomes increasingly critical as more  
430 renewable capacity is integrated into the system.

431 Future work is planned to extend the current analysis. First, climate

432 projection data will be integrated with different energy scenarios, incorpo-  
433 rating the addition of offshore wind, to better understand how climate change  
434 might affect RES droughts. Second, expanding the geographic domain of the  
435 study to include the rest of Europe would provide a more comprehensive un-  
436 derstanding of RES droughts in an interconnected energy grid. This would  
437 require extensive verification across other European countries, making it a  
438 more complex but highly relevant challenge.

## 439 Data Availability

440 The ERA5 data can be obtained from the Climate Data Store (<https://doi.org/10.24381/cds.adbb2d47>). The C3S-E dataset is also available  
441 from the Climate Data Store (<https://doi.org/10.24381/cds.4bd77450>).  
442 Information on wind and PV farms in Ireland can be obtained from the  
443 EirGrid website ([https://www.eirgrid.ie/grid/system-and-renewable](https://www.eirgrid.ie/grid/system-and-renewable-data-reports)  
444 [-data-reports](https://www.eirgrid.ie/grid/system-and-renewable-data-reports)). The Atlite model used in this study is open-source and can  
445 be found on GitHub (<https://github.com/pypsa/atlite>). The data and  
446 code required to reproduce the analysis in this article will be made available  
447 upon acceptance of the manuscript in a public GitHub repository.

## 449 Acknowledgments

450 The research conducted in this publication was funded by Science Foun-  
451 dation Ireland and co-funding partners under grant number 21/SPP/3756  
452 through the NexSys Strategic Partnership Programme.

## 453 References

- 454 [1] EuroStat, Renewable Energy Statistics, 2023. URL: [https://ec.europa.eu/eurostat/statistics-explained/index.php?title=Renewable](https://ec.europa.eu/eurostat/statistics-explained/index.php?title=Renewable_energy_statistics)  
455 [energy\\_statistics](https://ec.europa.eu/eurostat/statistics-explained/index.php?title=Renewable_energy_statistics), Accessed: 2024-11-06.
- 457 [2] H. C. Bloomfield, D. J. Brayshaw, L. C. Shaffrey, P. J. Coker, H. E.  
458 Thornton, Quantifying the increasing sensitivity of power systems to  
459 climate variability, *Environmental Research Letters* 11 (2016) 124025.  
460 doi:10.1088/1748-9326/11/12/124025.
- 461 [3] H. C. Bloomfield, D. J. Brayshaw, A. Troccoli, C. M. Goodess, M. De Fe-  
462 lice, L. Dubus, P. E. Bett, Y.-M. Saint-Drenan, Quantifying the

- sensitivity of european power systems to energy scenarios and climate change projections, *Renewable Energy* 164 (2021) 1062–1075. doi:10.1016/j.renene.2020.09.125.
- [4] K. van der Wiel, L. P. Stoop, B. R. H. Van Zuijlen, R. Blackport, M. A. Van den Broek, F. M. Selten, Meteorological conditions leading to extreme low variable renewable energy production and extreme high energy shortfall, *Renewable and Sustainable Energy Reviews* 111 (2019) 261–275. doi:10.1016/j.rser.2019.04.065.
- [5] F. Kaspar, M. Borsche, U. Pfeifroth, J. Trentmann, J. Drücke, P. Becker, A climatological assessment of balancing effects and shortfall risks of photovoltaics and wind energy in germany and europe, *Advances in Science and Research* 16 (2019) 119–128. doi:10.5194/asr-16-119-2019.
- [6] M. Ohba, Y. Kanno, D. Nohara, Climatology of dark doldrums in japan, *Renewable and Sustainable Energy Reviews* 155 (2022) 111927. doi:10.1016/j.rser.2021.111927.
- [7] F. Mockert, C. M. Grams, T. Brown, F. Neumann, Meteorological conditions during periods of low wind speed and insolation in Germany: The role of weather regimes, *Meteorological Applications* 30 (2023) e2141. doi:10.1002/met.2141.
- [8] M. J. Mayer, B. Biró, B. Szücs, A. Aszódi, Probabilistic modeling of future electricity systems with high renewable energy penetration using machine learning, *Applied Energy* 336 (2023) 120801. doi:10.1016/j.apenergy.2023.120801.
- [9] D. Raynaud, B. Hingray, B. François, J. Creutin, Energy droughts from variable renewable energy sources in European climates, *Renewable Energy* 125 (2018) 578–589. doi:https://doi.org/10.1016/j.renene.2018.02.130.
- [10] K. Z. Rinaldi, J. A. Dowling, T. H. Ruggles, K. Caldeira, N. S. Lewis, Wind and Solar Resource Droughts in California Highlight the Benefits of Long-Term Storage and Integration with the Western Interconnect, *Environmental Science and Technology* 55 (2021) 6214–6226. doi:10.1021/acs.est.0c07848.

- 496 [11] A. Gangopadhyay, A. K. Seshadri, N. J. Sparks, R. Toumi, The role  
497 of wind-solar hybrid plants in mitigating renewable energy-droughts,  
498 Renewable Energy 194 (2022) 926–937. doi:10.1016/j.renene.2022.  
499 05.122.
- 500 [12] S. Allen, N. Otero, Standardised indices to monitor energy droughts,  
501 Renewable Energy 217 (2023) 119206. doi:10.1016/j.renene.2023.11  
502 9206.
- 503 [13] J. Kapica, J. Jurasz, F. A. Canales, H. Bloomfield, M. Guezgouz,  
504 M. De Felice, Z. Kobus, The potential impact of climate change on  
505 european renewable energy droughts, Renewable and Sustainable En-  
506 ergy Reviews 189 (2024) 114011. doi:10.1016/j.rser.2023.114011.
- 507 [14] C. Bracken, N. Voisin, C. D. Burleyson, A. M. Campbell, Z. J. Hou,  
508 D. Broman, Standardized benchmark of historical compound wind and  
509 solar energy droughts across the Continental United States, Renewable  
510 Energy 220 (2024) 119550. doi:[https://doi.org/10.1016/j.renene](https://doi.org/10.1016/j.renene.2023.119550)  
511 .2023.119550.
- 512 [15] H. Hersbach, B. Bell, P. Berrisford, S. Hirahara, A. Horányi, J. Muñoz-  
513 Sabater, J. Nicolas, C. Peubey, R. Radu, D. Schepers, et al., The ERA5  
514 global reanalysis, Quarterly Journal of the Royal Meteorological Society  
515 146 (2020) 1999–2049. doi:10.1002/qj.3803.
- 516 [16] L. Dubus, Y. Saint-Drenan, A. Troccoli, M. De Felice, Y. Moreau, L. Ho-  
517 Tran, C. Goodess, R. Amaro E Silva, L. Sanger, C3S Energy: A climate  
518 service for the provision of power supply and demand indicators for Eu-  
519 rope based on the ERA5 reanalysis and ENTSO-E data, Meteorological  
520 Applications 30 (2023) e2145. doi:10.1002/met.2145.
- 521 [17] Copernicus Climate Change Service (C3S), Climate and energy indi-  
522 cators for Europe from 1979 to present derived from reanalysis., 2020.  
523 doi:10.24381/cds.4bd77450, accessed on 28-11-2024.
- 524 [18] F. Hofmann, J. Hampp, F. Neumann, T. Brown, J. Hörsch, Atlite: a  
525 lightweight Python package for calculating renewable power potentials  
526 and time series, Journal of Open Source Software 6 (2021) 3294. doi:10  
527 .21105/joss.03294.

- [19] J. Li, Z. Zhao, D. Xu, P. Li, Y. Liu, M. A. Mahmud, D. Chen, The potential assessment of pump hydro energy storage to reduce renewable curtailment and CO2 emissions in Northwest China, *Renewable Energy* 212 (2023) 82–96. doi:10.1016/j.renene.2023.04.132.
- [20] M. Parzen, H. Abdel-Khalek, E. Fedotova, M. Mahmood, M. M. Frysztacki, J. Hampp, L. Franken, L. Schumm, F. Neumann, D. Poli, et al., Pypsa-earth. a new global open energy system optimization model demonstrated in africa, *Applied Energy* 341 (2023) 121096. doi:10.1016/j.apenergy.2023.121096.
- [21] K. Ali Khan Niazi, M. Victoria, Comparative analysis of photovoltaic configurations for agrivoltaic systems in europe, *Progress in Photovoltaics: Research and Applications* 31 (2023) 1101–1113. doi:10.1002/pip.3727.
- [22] EirGrid & SONI, System and Renewable Data Reports, 2023. URL: <https://www.eirgrid.ie/grid/system-and-renewable-data-reports>, Accessed: 2024-11-06.
- [23] P. T. Brown, D. J. Farnham, K. Caldeira, Meteorology and climatology of historical weekly wind and solar power resource droughts over western North America in ERA5, *SN Applied Sciences* 3 (2021) 814. doi:10.1007/s42452-021-04794-z.
- [24] N. Otero, O. Martius, S. Allen, H. Bloomfield, B. Schaeffli, Characterizing renewable energy compound events across Europe using a logistic regression-based approach, *Meteorological Applications* 29 (2022) e2089. doi:10.1002/met.2089, 13.
- [25] Y.-M. Saint-Drenan, L. Wald, T. Ranchin, L. Dubus, A. Troccoli, An approach for the estimation of the aggregated photovoltaic power generated in several European countries from meteorological data, *Advances in Science and Research* 15 (2018) 51–62. doi:10.5194/asr-15-51-2018.
- [26] I. Staffell, S. Pfenninger, Using bias-corrected reanalysis to simulate current and future wind power output, *Energy* 114 (2016) 1224–1239. doi:10.1016/j.energy.2016.08.068.

- 560 [27] Government of Ireland, Climate Action Plan 2024, Technical Report 3,  
561 Department of the Environment, Climate and Communications, 2023.  
562 URL: [https://www.gov.ie/pdf/?file=https://assets.gov.ie/](https://www.gov.ie/pdf/?file=https://assets.gov.ie/284675/70922dc5-1480-4c2e-830e-295afd0b5356.pdf)  
563 [284675/70922dc5-1480-4c2e-830e-295afd0b5356.pdf](https://www.gov.ie/pdf/?file=https://assets.gov.ie/284675/70922dc5-1480-4c2e-830e-295afd0b5356.pdf), Accessed:  
564 2024-11-06.
- 565 [28] Sustainable Energy Authority Ireland, National Energy Projections  
566 2024, Technical Report, Sustainability Energy Authority of Ireland,  
567 2024. URL: [https://www.seai.ie/news-and-events/news/energ](https://www.seai.ie/news-and-events/news/energy-projections-report)  
568 [y-projections-report](https://www.seai.ie/news-and-events/news/energy-projections-report), Accessed: 2024-11-06.
- 569 [29] H. G. Beyer, G. Heilscher, S. Bofinger, A robust model for the mpp  
570 performance of different types of pv-modules applied for the performance  
571 check of grid connected systems, Eurosun (2004) 8.